Hindawi
International Journal of Rotating Machinery
Volume 2023, Article ID 5692229, 14 pages
https://doi.org/10.1155/2023/5692229

Research Article

Effect of Multifactor Interaction on the Accuracy of RV Reducers

Zihui Wang,[1,2] Rui Xu,[1,2,3] Jiabao Pan,[1,3] Qingqing Chen,[1,2] Jing Zhang,[4] and Jiugen Wang[5]

[1]*School of Mechanical Engineering, Anhui Polytechnic University, Wuhu 241000, China*
[2]*Wuhu Ahpu Robot Technology Research Institute Co., Ltd., Wuhu 241000, China*
[3]*National Key Laboratory of Science and Technology on Helicopter Transmission, Nanjing University of Aeronautics and Astronautics, Nanjing 210016, China*
[4]*Zhejiang Fine Motion Robot Joint Technology Co., Ltd., Yuhuan 317600, China*
[5]*School of Mechanical Engineering, Zhejiang University, Hangzhou 310058, China*

Correspondence should be addressed to Rui Xu; xurui@ahpu.edu.cn

Received 30 December 2022; Revised 21 June 2023; Accepted 27 June 2023; Published 13 July 2023

Academic Editor: Ashwani K. Gupta

The rotary vector (RV) reducer is one of the widely used mechanical components in industrial systems, specifically in robots. The stability of the transmission performance of the RV reducer is crucial for the efficient operation of industrial equipment. The manufacturing and assembly errors of various components of the RV reducer during the production process are important factors that affect the transmission performance. However, in previous research work, the coupling effect of multiple errors on the transmission accuracy of RV reducer has not been fully considered. Furthermore, a vague relationship between system transmission errors and various errors also has not been thoroughly discussed, which presents a challenge to analyze and optimize the errors of components using the simulation technology of virtual prototype. Therefore, we propose a novel approach to use the response surface method (RSM) to investigate the transmission accuracy of RV reducer. Firstly, based on the constructed virtual prototype of RV reducer, the individual effects of different original errors on the overall transmission error are analyzed. Secondly, a response surface approximation model using RSM is constructed to analyze the effect of multiple error interactions on the transmission accuracy of the RV reducer, and the potential functional relationship between multiple error factors and the overall transmission error is also explored. Finally, the authenticity of the proposed approach is verified by setting up some comparative experiments. This study provides a reference for the efficient analysis and optimization of the transmission accuracy of RV reducers.

1. Introduction

Rotary vector (RV) reducer is a secondary transmission component derived from cycloid-pin gear transmission and is widely used for precision mechanical systems owing to its characteristics of high rigidity, large transmission ratio, high transmission accuracy, high transmission efficiency, and compact structure [1, 2]. The stability of the transmission performance of the RV reducer is crucial for the efficient operation of the equipment.

In order to design high performance of RV reducers, many researchers have conducted extensive research on performance analysis. Xu [3] proposed a dynamic model to accurately predict the number of pinwheels for load transfer in an RV reducer with assembly clearance to improve transmission performance. On the basis of the analysis of the response sensitivity of cyclic symmetric structure, Yang et al. [4] developed a kinetic model to investigate the effects of the dynamic characteristics of RV reducer on its performance. Xu et al. [5] developed a dynamic model for the bearing-cycloid-pinwheel transmission mechanism in an RV reducer and analyzed the transfer characteristics and dynamic contact response. Wang et al. [6] proposed a new multitooth contact model and a TE model of an RV reducer and studied the influence of load on the different modification methods. As an important and effective analysis method, the virtual prototype simulation technology is also frequently used in the analysis of RV reducers, which can

simplify the analysis process and improve the effectiveness of the analysis. Jin et al. [7] utilized virtual prototype technology to investigate the main factors affecting the dynamic transmission error of an RV reducer and analyzed the error transmission relationship of the RV reducer. Zhang et al. [8] constructed a virtual prototype of an RV reducer based on multibody dynamic theory to study the effect of changing the clearance among the cycloid gear and pin, the crankshaft, and the bearing on the transmission error of the RV reducer. To keep the long-term stability of transmission performance, a lot of research work about the fault detection of robot reducer has also been done. Qian et al. [9] proposed a time-variant reliability method for multiple failure modes based on a double-loop Kriging model. Raouf et al. [10] introduced a novel approach to use the embedded electrical current system for the fault detection of the RV reducer, which provides new ideas and important references for the fault detection of reducers. In the study, they presented an approach for feature extraction, feature selection, and feature reduction using the information obtained from the motor current signature analysis to create an ML-based fault classification system with distinguishable prominent features. The research group [11] also provided a robust approach to utilize the embedded setup of the electrical current for the fault detection of the robotic strain wave gear reducer based on variable speed of operation. These studies have laid an important foundation for improving the performance of robot reducers.

The manufacturing and assembly errors during production process of various components of the RV reducer are also another important factor that needs to be noted, as they may have a significant impact on the transmission accuracy of the RV reducer due to its complicated structure [12–14]. So, for this reason, many studies have also been conducted on the actual effects of different errors on the transmission accuracy of RV reducers. Blanche and Yang [15, 16] developed an analytical model of tooth side clearance with machining deviations and investigated the effects of periodic changes in tooth clearance and torque pulsation on transmission accuracy. Ahn et al. [17] used finite element method to analyze the effects of tolerance and friction between the cycloid disk and pin on the performance of an RV reducer. Jiang et al. [18] predicted the reliability of RV reducers in view of the uncertainty of manufacturing and assembly errors and explored the effect of error randomness on their dynamic transmission characteristics. Yang et al. [19] proposed an error analysis modeling method through an established kinematic equivalent mechanism to study the effects of raw errors on transmission accuracy at high and low speed stages. Hu et al. [20] proposed an elastic transmission error compensation method to determine the error factors that positively affect the transmission error to reduce the elastic error of an RV reducer.

These literatures point out the direction and provide important references for analyzing and optimizing the error parameters of RV reducers. However, in previous literatures, the coupling effect of multiple errors on the transmission accuracy of RV reducer has not been fully considered. Furthermore, because of the complexity of RV reducer and its transmission, a vague relationship between the system transmission errors and various errors also has not been thoroughly discussed, which presents a challenge to analyze and optimize the errors of components using the simulation technology of virtual prototype. Therefore, we propose a novel approach to use the response surface method (RSM) to investigate the transmission accuracy of RV reducer. RSM is a statistical method for solving multivariable problems. It is based on a reasonable experimental design method, which obtains certain data through experiments and uses multiple quadratic regression equations to fit the functional relationship between factors and response values. On the basis of this model, the relationship between the response target and each design variable can be determined, which will greatly simplify the analysis process and save calculation time. Especially when dealing with complex systems, approximate models can be used to dynamically observe changes in the target at any time to intuitively understand the detailed impact of local factors on the overall system. Compared with the existing method, the advantage of RSM can obtain an approximate relationship between factors and response objectives based on fewer experiments, and this relationship can be expressed using explicit functions, which can effectively improve the efficiency of system analysis and optimization design. Therefore, RSM has been widely applied in various fields. Schleich and Wartzack [21] constructed a quadratic regression model with

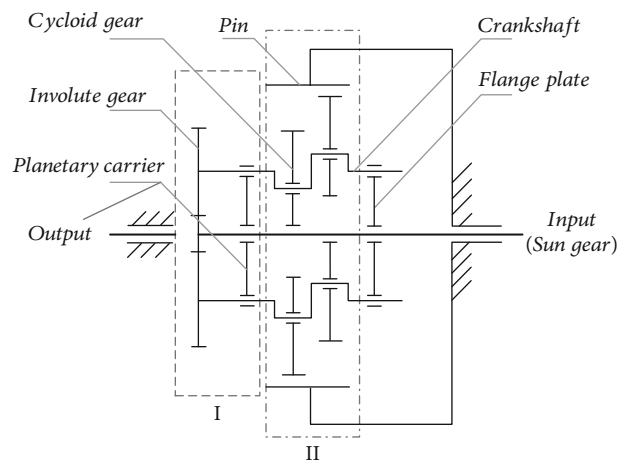

Figure 1: Transmission schematic of RV reducer.

Table 1: Basic structural parameters of RV reducer.

Parameter	Parameter value	Unit
Number of teeth of sun gear	12	/
Number of teeth of involute gear	36	/
Number of teeth of pin	40	/
Number of teeth of cycloid gear	39	/
Transmission ratio (i)	121	/
Radius of pin	6	mm
Diameter of distribution circle of pin	128	mm
Eccentricity of cycloid gear	1.3	mm

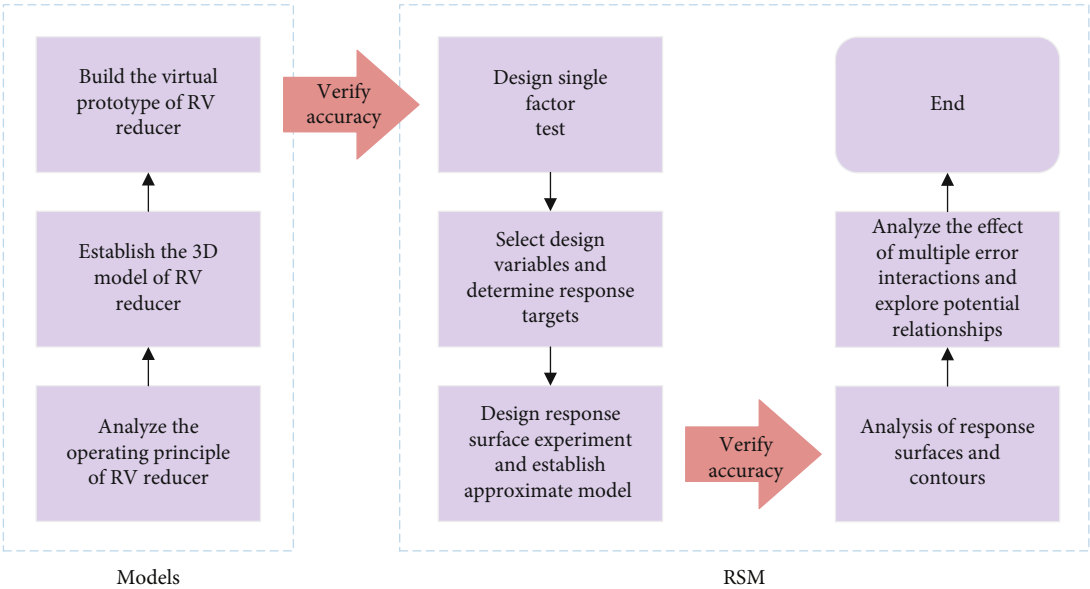

Figure 2: Overall workflow.

interaction using RSM to quantify the correlation between input and output parameters in tolerance analysis. Nguyen and Duy [22] used the RSM of Behnken to study the influence of geometric and working parameters on the efficiency of gear transmission. Previously, the authors [23] studied the tolerance analysis modeling approach for gears based on RSM and small displacement torsor method to build a response surface approximate model between gear tolerance variable elements and transmission errors.

Considering the complexity of numerical simulation of RV reducer and the advantages of RSM method in constructing fitting models, RSM is introduced to investigate the transmission accuracy of RV reducer in this paper. To analyze the effect of multiple error interactions on the transmission accuracy of the RV reducer, we use RSM for experimental design, with the multiple error factors as the design variables and the transmission accuracy as the response target. On the basis of experimental data, a response surface approximation model is constructed to analyze the effect of multiple error interactions on the transmission accuracy of the RV reducer and explore the potential functional relationship between multiple error factors and the overall transmission error. And the authenticity of the proposed approach also is verified by setting up some comparative experiments.

2. Principle and Methods

The architecture of a certain type of RV reducer is shown in Figure 1. The RV reducer is divided into two stages of reduction, consisting of an involute gear reduction mechanism in stage I and a cycloid-pin gear reduction mechanism in stage II. When the pin housing is fixed, the input shaft (sun gear) is used as the input of the reduction mechanism in stage I, and if it rotates in the clockwise direction, then the involute gear rotates counterclockwise. At this time, the two crankshafts, which are offset in the same direction and fixed to the involute gear, rotate counterclockwise with the involute gear and drive the two cycloid gears with a phase difference of 180° to rotate. The cycloid gear drives the crankshaft to rotate in clockwise direction by meshing with the pin, and it is used as the input of the reduction mechanism in stage II. The output motion is realized by the clockwise rotation of the output disk (planetary carrier).

The basic structural parameters of this RV reducer are shown in Table 1.

This paper mainly studies the transmission accuracy of RV reducer based on RSM, and the overall process is shown in Figure 2.

3. Usability Analysis of Virtual Prototype Simulation of RV Reducer

3.1. 3D Designed Model of RV Reducer. SolidWorks (version 2020) is utilized to draw the modules of the RV reducer and model assembly. On the premise of ensuring the accuracy of simulation analysis, the 3D model of the RV reducer is simplified. The fine geometric features that do not affect the simulation results, such as chamfers, fillets, threads, and other features, are removed, and fasteners, such as bolts and pins, are ignored to reduce the system's computational workload and improve the computational speed. The complete model of the assembled RV reducer is shown in Figure 3(a), and the exploded view of its simplified model is shown in Figure 3(b). To ensure that the 3D model of the RV reducer can be smoothly imported into ADAMS software (version 2020) for dynamic simulation, the 3D model is checked for dynamic and static interference of parts to ensure the absence of interference within the model.

3.2. Analyzed Virtual Prototype of RV Reducer

3.2.1. Initial Imported Parameters. The solid model of the RV reducer is imported into the ADAMS software. The unit

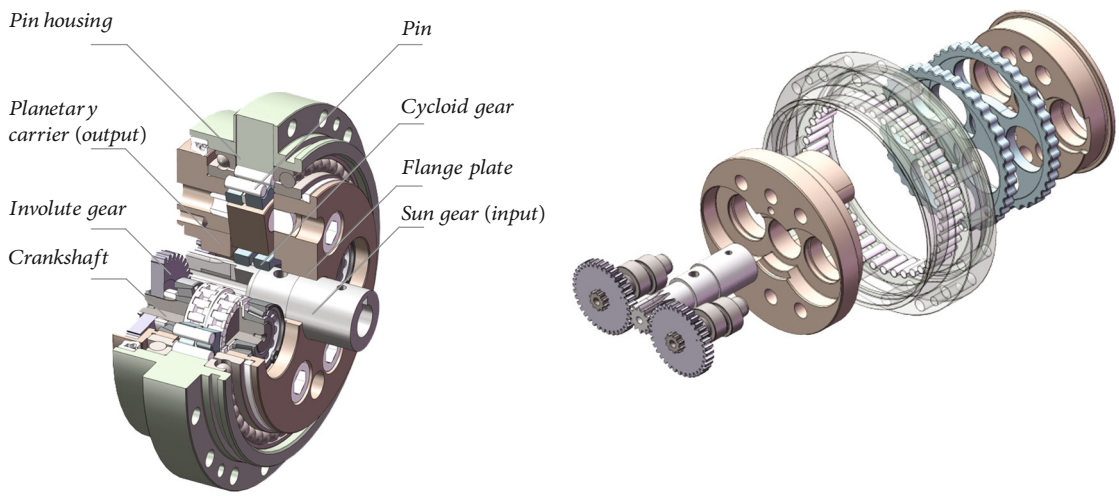

(a) (b)

Figure 3: 3D model of RV reducer. (a) The complete model of the assembled RV reducer. (b) The exploded view of the simplified model.

Table 2: Material properties of the parts of the RV reducer.

Parameter	Material	Elastic modulus (E/(N·m^{-2}))	Density (ρ/(kg·m^{-3}))	Poisson's ratio
Sun gear	15CrMo	2.12×10^{11}	7.88×10^{3}	0.284
Involute gear	38CrMoAl	2.11×10^{11}	7.85×10^{3}	0.277
Crankshaft	20CrMnMo	2.07×10^{11}	7.87×10^{3}	0.254
Planetary carrier	ZG65Mn	1.98×10^{11}	7.85×10^{3}	0.230
Pin gear housing	QT500-7	1.68×10^{11}	7.25×10^{3}	0.240
Pin gear	GCr15	2.19×10^{11}	7.83×10^{3}	0.300
Cycloid gear	20CrMnMo	2.07×10^{11}	7.87×10^{3}	0.254
Flange plate	ZG65Mn	1.98×10^{11}	7.85×10^{3}	0.230

system is set to MMKS (length in millimeters, mass in kilograms, and time in seconds), and the gravity direction is set to the Y-axis. Then, the appropriate working grid interval and material properties of each part are defined. The material properties are shown in Table 2.

3.2.2. Constraint of the RV Model. According to the transmission principle of the RV reducer, constraints are added to its components, and the kinematic pair among the components is accurately defined. The constraints are set, as shown in Table 3. To ensure that the real operation of the RV reducer is simulated, the constraint between the sun gear and the involute gear is set to contact. If a gear pair (coupling pair) is used, the relative rotation speed between the master and driven gears will remain fixed, and deviations will be present from the real operation.

The contact force function in ADAMS is used to simulate the interaction forces between gears. The contact force of the involute gear drive and cycloid-pin gear drive is defined by impact function-based contact. It includes the elastic force generated by the two components cutting into each other and the damping force generated by the relative velocity [24, 25]. The impact function expression is

Table 3: Constraint relations of each component of the RV reducer.

Type of constraint	Part 1	Part 2
Fixed joint	Pin housing	Ground
Fixed joint	Pin	Pin housing
Fixed joint	Involute gear	Crankshaft
Fixed joint	Planetary carrier	Flange plate
Revolute joint	Sun gear	Ground
Revolute joint	Crankshaft	Planetary carrier
Revolute joint	Cycloid gear	Crankshaft
Revolute joint	Planetary carrier	Ground
Contact pair	Pin	Cycloid gear
Contact pair	Sun gear	Involute gear

$$\text{IMPACT} = \begin{cases} K(q_1 - q)^e - C_{\max}\bar{q} * \text{step}\,(q, q_1, -d, 1, q_1, 0), & q < q_1, \\ 0, & q > q_1, \end{cases} \tag{1}$$

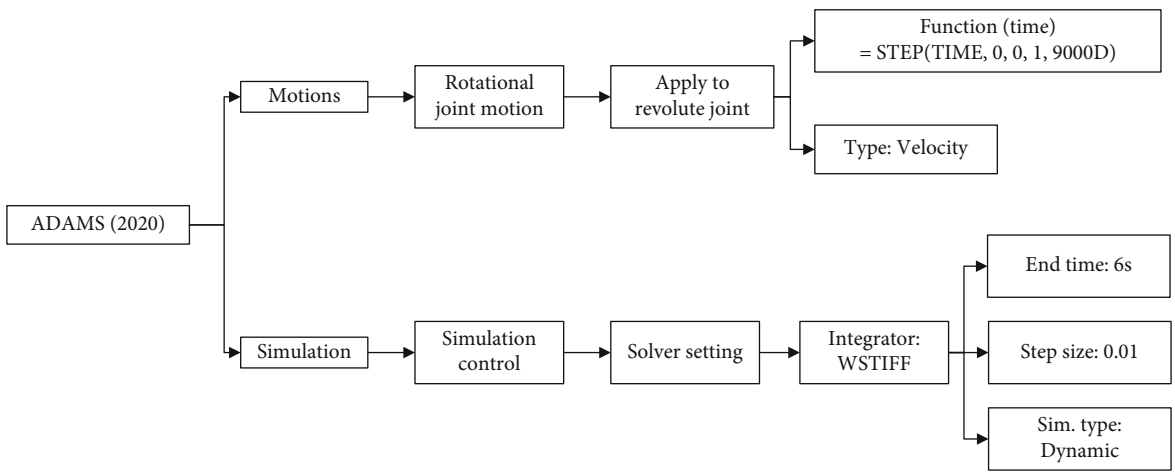

Figure 4: Related definitions within ADAMS.

where q is the distance between two contact objects, $\bar{q}$ is the velocity between two objects in contact, q_1 is the threshold value of the impact function, K is the stiffness coefficient, e is the impact force index, $C_{\max}$ is the maximum damping coefficient, and d is the distance traveled when the damping reaches the maximum value.

3.2.3. Setting the Speed and Solving the Parameters of the Analyzed Model. The drive is added to the revolution of the input shaft. To avoid the speed surge generated by the RV reducer in the start-up phase due to instantaneous loading, the drive function is defined by choosing a step function, and the speed of the input is smoothly increased from 0°/s to 9000°/s (1500 r/min) in 0 s to 1 s by using the type of velocity and is then kept stable. The function is expressed as follows: Function(time) = STEP(TIME, 0, 0, 1, 9000D).

After the model-related definitions are set, the model is verified to pass, the simulation type is selected as dynamic simulation, the solver is selected as WSTIFF, the simulation time is set to 6 s, and the step size is 0.01. The above definitions are set up within ADAMS, as shown in Figure 4.

The virtual prototype of the RV reducer created by the above steps is shown in Figure 5.

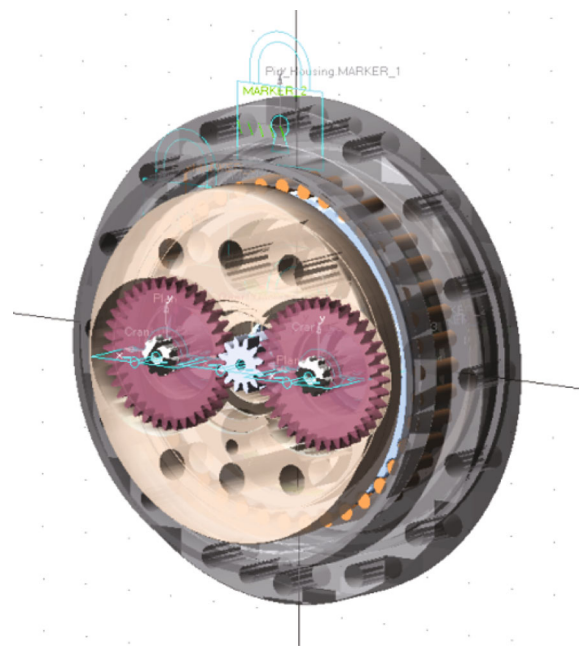

Figure 5: Virtual prototype of the RV reducer.

3.3. Validation of Availability. The input shaft speed and output disk speed of the virtual prototype of the RV reducer are shown in Figure 6. The input shaft angular speed reaches the stable speed at 1 s. The output disk operation pattern is the same as the input shaft, and it runs for one cycle from 1 s to 6 s with an average speed of 74.43°/s. The actual transmission ratio of the virtual prototype is 120.92, which is consistent with the theoretical transmission ratio.

The angular errors of the RV reducer can visually reflect its transmission accuracy, and the difference between the actual output angle and the theoretical output angle (actual input angle/i) is the angular error.

The transmission error curve of the virtual prototype of the RV reducer is shown in Figure 7. Particularly, the transmission error range is $-0.4344'$ to $0.4174'$ for one cycle of output disk operation. This result indicates that the error between the simulation result and the theoretical value is within a reasonable range. This finding verifies the consistency of the established virtual prototype of RV reducer compared with the RV reducer in the actual moving process and the usability of the virtual prototype.

4. Construction of Transmission Error Response Surface Model

4.1. Principles of RSM. RSM is an approach for constructing an approximate model that simulates the true response surface by fitting a global approximation of the output variables (system response) to a design of experiments at test points in a specified design space [26].

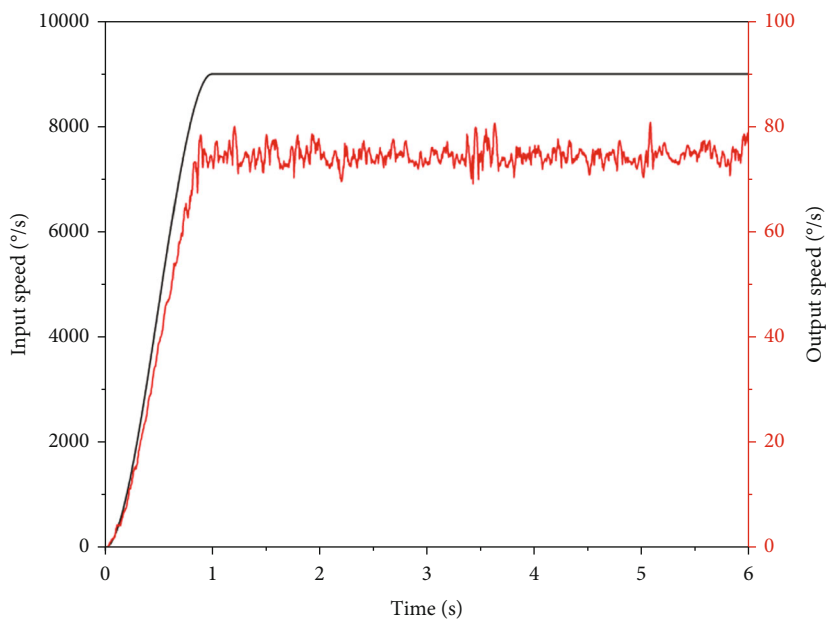

Figure 6: Input and output speed of the virtual prototype.

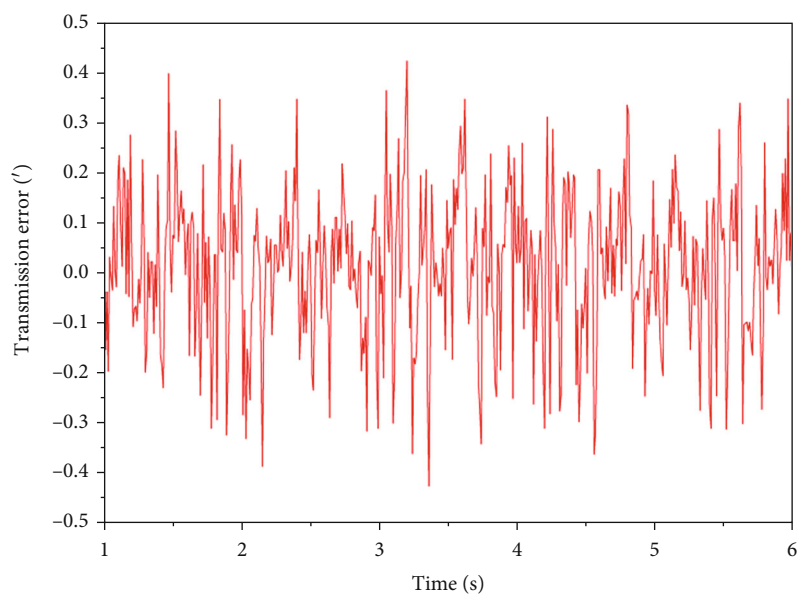

Figure 7: Transmission error of the virtual prototype of the RV reducer.

The following equation is satisfied between the system response objectives and the design variables:

$$Y = \bar{y}(x) + \delta, \tag{2}$$

where $\bar{y}(x)$ is the approximate function of the original function $y(x)$, that is, the response surface, and δ is the total error.

The response surface can be defined as follows:

$$\bar{y}(x) = \alpha_0 + \sum_{i=1}^{N} \alpha_i \varphi_i(x), \tag{3}$$

where α_0 is the offset term, $\varphi_i(x)$ is the basis function, α_i is the coefficient of the basis function, and N is the number of basis functions, which leads to the following second-order response surface approximation function:

$$\bar{y}(x) = \alpha_0 + \sum_{i=1}^{N} \alpha_i x_i + \sum_{i=1}^{N} \alpha_{ii} x_i^2 + \sum_{1=i<j}^{N} \alpha_{ij} x_i x_j, \tag{4}$$

where α_0 is the offset term, α_i is the linear offset term, α_{ii} is the second-order offset coefficient, and α_{ij} is the interaction coefficient.

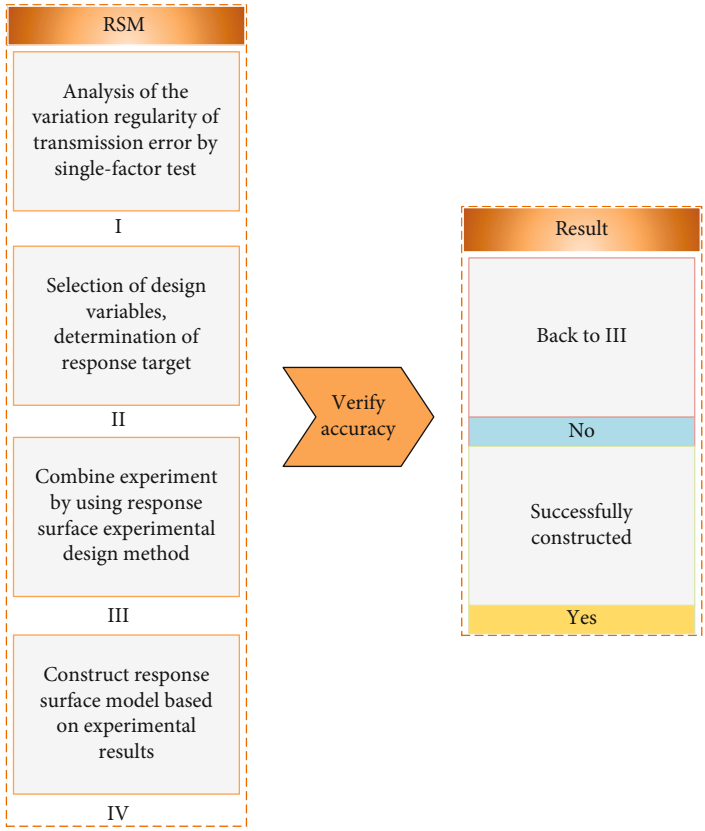

Figure 8: Construction of the response surface model.

Table 4: Types of single-factor error.

Symbol	Types of error	Initial value (+)
Ⓐ	None	0
Ⓑ	Eccentricity error of sun gear assembly	10 μm
Ⓒ	Eccentricity error of involute gear assembly	10 μm
Ⓓ	Phase error of cam segment on crankshaft	10 μm
Ⓔ	Eccentricity error of cam segment on crankshaft	10 μm
Ⓕ	Eccentricity error of crankshaft hole of planetary carrier	10 μm
Ⓖ	Eccentricity error of crankshaft hole of cycloid gear (E_D)	10 μm
Ⓗ	Circumferential position error of distribution circle of pin	10 μm
Ⓘ	Error of pin distribution circle diameter (E_B)	10 μm
Ⓙ	Error of pin radius (E_C)	5 μm
Ⓚ	Phase error of cycloid gear	0.1°
Ⓛ	Deviation of pin pitch (E_A)	0.01°

The matrix of coefficients of the basis functions is calculated using the least squares method, shown as follows:

$$\boldsymbol{\beta} = \left(\boldsymbol{\theta}^T\boldsymbol{\theta}\right)^{-1}\boldsymbol{\theta}^T\boldsymbol{Y}, \tag{5}$$

where $\boldsymbol{\theta}$ is the response surface sample point matrix, which can be expressed as

$$\boldsymbol{\theta} = \begin{pmatrix} 1 & x_{1,1} & x_{1,2} & \cdots & x_{1,J} \\ 1 & x_{2,1} & x_{2,2} & \cdots & x_{2,J} \\ \vdots & \vdots & \vdots & & \vdots \\ 1 & x_{I,1} & x_{I,2} & \cdots & x_{I,J} \end{pmatrix}. \tag{6}$$

Then, $\boldsymbol{Y}$ is the response vector corresponding to the design sample points, that is,

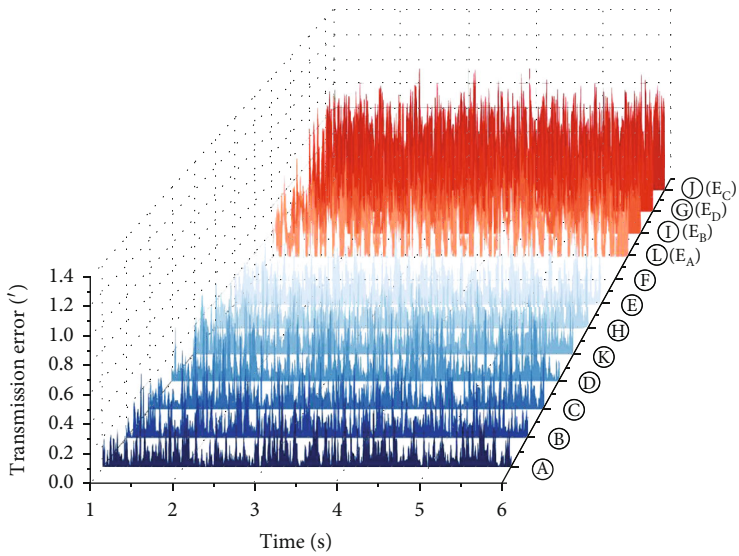

Figure 9: Influence of single-factor error on the transmission accuracy of the RV reducer.

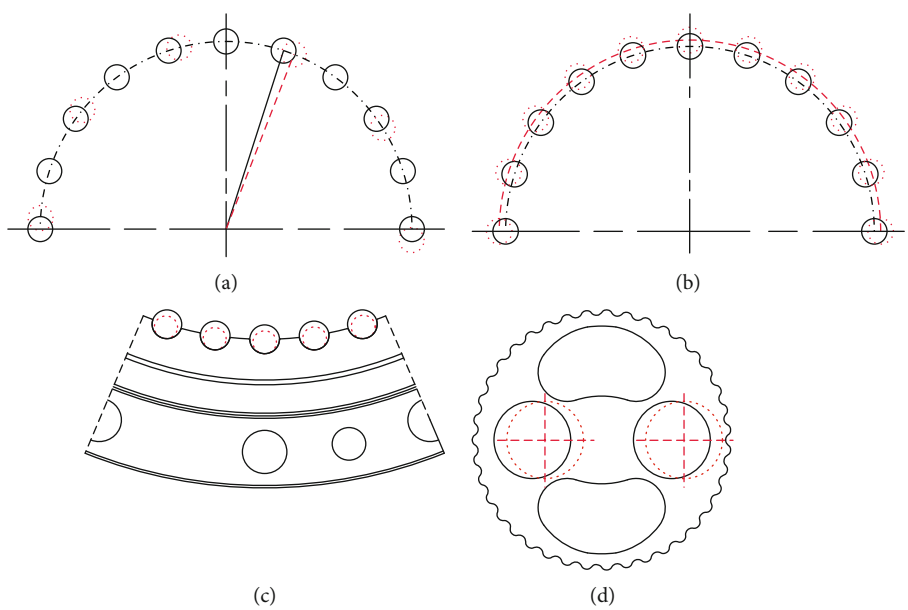

Figure 10: Schematic of error types. (a) The deviation of pin pitch. (b) The error of pin distribution circle diameter. (c) The error of pin radius. (d) The eccentricity error of the crankshaft hole of the cycloid gear.

$$\boldsymbol{Y} = (y_1, y_2, \cdots, y_I)^T. \tag{7}$$

By determining $\boldsymbol{\theta}$ and $\boldsymbol{Y}$ according to the design sample points and obtaining the coefficient matrix $\boldsymbol{\beta}$, the specific functional expressions corresponding to the response surface can be determined.

4.2. Design of Response Surface Experiments. On the basis of the established virtual prototype of the RV reducer, a model including multiple single-factor error types is set up to explore their effects on the transmission accuracy of the RV reducer. The main error factors are selected as different design sample points to further investigate the influence of the interaction on multiple errors. In this manner, the response surface model of the RV reducer's transmission error can be established, and the specific steps are as follows:

(1) The design variables and response targets are determined. In this paper, the main error factors are the following: deviation of pin pitch (E_A), error of the pin distribution circle diameter (E_B), error of the pin radius (E_C), and eccentricity error of the crankshaft hole of the cycloid gear (E_D). The RV reducer transmission error is set as the response target

(2) For the design method, a single-factor test is used to screen the main error factors, and the Box-

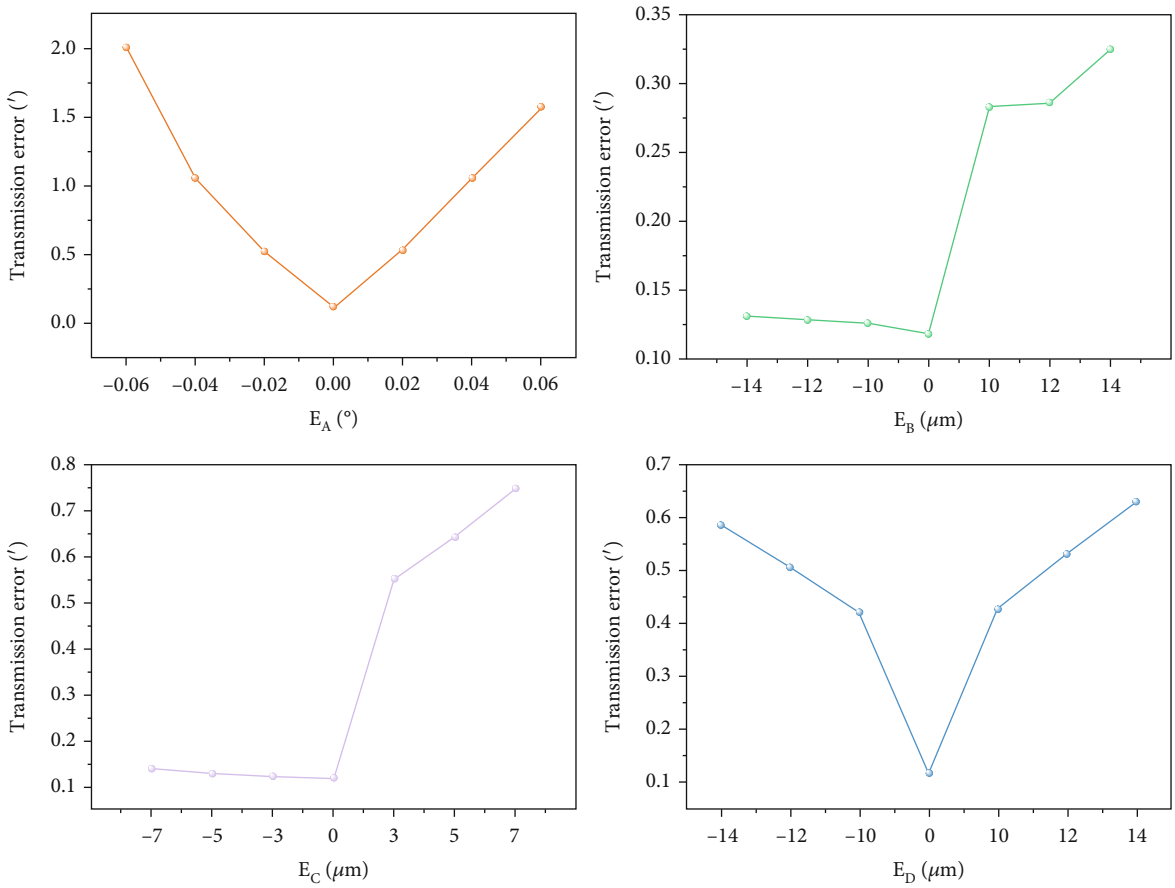

Figure 11: Trend of transmission error.

Table 5: Design factors and levels of response surface experiments.

Factor	Variable	Level		
		−1	0	1
Deviation of pin pitch (°)	E_A	−0.06	0	0.06
Error of pin distribution circle diameter (μm)	E_B	−14	0	14
Error of pin radius (μm)	E_C	−7	0	7
Eccentricity error of crankshaft hole of cycloid gear (μm)	E_D	−14	0	14

Behnken matrix sampling method is used to take three levels for each factor, coded as (−1, 0, 1), corresponding to the low, intermediate, and high values at the experimental sites, respectively. And a combination test is conducted according to each factor level [27]

(3) The response surface model is constructed, and its accuracy is verified. Particularly, the response surface model of the objective function is constructed by combining the above experimental design, and the analysis of variance and significance test are performed to verify its accuracy [28]

The construction of the response surface model of the transmission error of the RV reducer is shown in Figure 8.

4.2.1. Single-Factor Tests. On the basis of the actual specifications of engineering manufacturing and assembly, the magnitude of the error of each factor is controlled within a reasonable range, and the level of the initial error is unified. The types and parameters of the error are shown in Table 4.

According to the types of error in Table 4, a model with errors is created using SolidWorks software. The model is converted into a solid format and then imported into ADAMS software for virtual prototype simulation and sequential analysis. On the basis of the simulation of experiment results, the influence curves of various types of single-factor error on the transmission error of RV reducer are obtained, as shown in Figure 9.

As shown in Figure 9, the error in the involute gear reduction mechanism in stage I has a minimal influence on the transmission accuracy of the RV reducer. The

Table 6: Design results of response surface experiments.

Number	E_A (°)	E_B (μm)	E_C (μm)	E_D (μm)	Mean value of transmission error ($\gamma/'$)
1	1	0	1	0	1.702960
2	−1	1	0	0	2.145570
3	0	1	0	1	0.582340
4	0	0	0	0	0.175502
5	0	−1	−1	0	0.306938
6	0	−1	0	−1	0.632792
7	−1	0	1	0	1.893480
8	0	−1	1	0	0.439095
9	0	0	0	0	0.104159
10	−1	0	−1	0	2.196420
11	0	0	−1	1	0.625511
12	0	0	−1	−1	0.616317
13	−1	−1	0	0	2.135760
14	1	0	0	−1	1.534670
15	1	0	−1	0	1.384840
16	0	1	−1	0	0.120106
17	1	0	0	1	1.546350
18	−1	0	0	1	2.038870
19	0	1	0	−1	0.574657
20	−1	0	0	−1	2.043050
21	0	−1	0	1	0.633850
22	0	1	1	0	1.137310
23	0	0	1	1	0.607289
24	1	1	0	0	1.646300
25	0	0	1	−1	0.650322
26	1	−1	0	0	1.431230
27	0	0	0	0	0.104159

disturbance generated by its error has been significantly reduced when it is transmitted to the output through the cycloid-pin gear reduction mechanism in stage II, whereas the error in the gear mechanism in stage II has a greater effect on the transmission accuracy of the RV reducer. Particularly, four error types, namely, E_A (a), E_B (b), E_C (c), and E_D (d), have an obvious influence on the RV reducer's transmission accuracy. And the types of error indication (in the positive direction for example) are shown in Figure 10.

The range of single-factor error values is increased, and the four error types are refined. And the mean value of the RV reducer's transmission error is used to evaluate the changing amplitude of transmission accuracy. The results of the single-factor error's variation are shown in Figure 11.

4.2.2. Factors and Levels of Response Surface Experiments. According to the results of the single-factor test, the optimal value of transmission error corresponding to each factor is set as the middle level. The design factor and corresponding levels of the response surface experiment are shown in Table 5.

Table 7: Analysis of variance for the response surface model.

Source	Sum of squares	DF	Mean square	F value	P value
Model	13.44	14	0.9598	37.93	<0.0001
E_A	0.8570	1	0.8570	33.86	<0.0001
E_B	0.0327	1	0.0327	1.29	0.2777
E_C	0.1161	1	0.1161	4.59	0.0534
E_D	0.0000	1	0.0000	0.0010	0.9750
E_AE_B	0.0105	1	0.0105	0.4162	0.5310
E_AE_C	0.0964	1	0.0964	3.81	0.0747
E_AE_D	0.0001	1	0.0001	0.0025	0.9611
E_BE_C	0.1958	1	0.1958	7.74	0.0166
E_BE_D	0.0000	1	0.0000	0.0004	0.9837
E_CE_D	0.0007	1	0.0007	0.0269	0.8723
${E_A}^2$	11.30	1	11.30	446.61	<0.0001
${E_B}^2$	0.2500	1	0.2500	9.88	0.0085
${E_C}^2$	0.2205	1	0.2205	8.72	0.0121
${E_D}^2$	0.3442	1	0.3442	13.60	0.0031
Residual	0.3037	12	0.0253	/	/
Lack of fit	0.3003	10	0.0300	17.70	0.0546
Pure error	0.0034	2	0.0017	/	/
Cor total	13.74	26	/	/	/

Note: significant, $P < 0.05$; highly significant, $P < 0.01$; $R^2 = 0.9779$; $R^2_{\text{adj}} = 0.9521$.

4.2.3. Construction of Response Surface Model and Evaluation of Accuracy. The experimental protocol and results of the multifactor combination are shown in Table 6.

According to the experimental results, the regression coefficient matrix is calculated by the least squares method, and the quadratic polynomial response surface function of the RV reducer's transmission error is constructed as

$$\begin{aligned}\gamma = {} & 0.12794 - 4.45389E_A + 3.73 \times 10^{-3}E_B + 1.4052 \times 10^{-2}E_C \\ & - 1.05 \times 10^{-4}E_D + 6.1089 \times 10^{-2}E_AE_B + 0.369675E_AE_C \\ & + 4.719 \times 10^{-3}E_AE_D + 2.258 \times 10^{-3}E_BE_C + 8.45057 \\ & \times 10^{-6}E_BE_D - 1.33 \times 10^{-4}E_CE_D + 4.0436592 \times 10^{2}{E_A}^2 \\ & + 1.105 \times 10^{-3}{E_B}^2 + 4.15 \times 10^{-3}{E_c}^2 + 1.296 \times 10^{-3}{E_D}^2.\end{aligned} \tag{8}$$

The results of the ANOVA and significance test for the constructed response surface model are shown in Table 7.

The significance of the terms in the ANOVA is an evaluation criteria for the model, and the more significant the parameter is, the greater the influence on the response target will be. As shown in Table 7, the model has a P value of <0.0001 (highly significant) when the RV reducer's transmission error is the response value, the lack of fit P value = 0.0546>0.05 (not significant), the determination coefficient $R^2 = 97.79\%$, and the adjusted determination coefficient $R^2_{\text{adj}} = 95.21\%$. The closeness of R^2 to 1 and the value

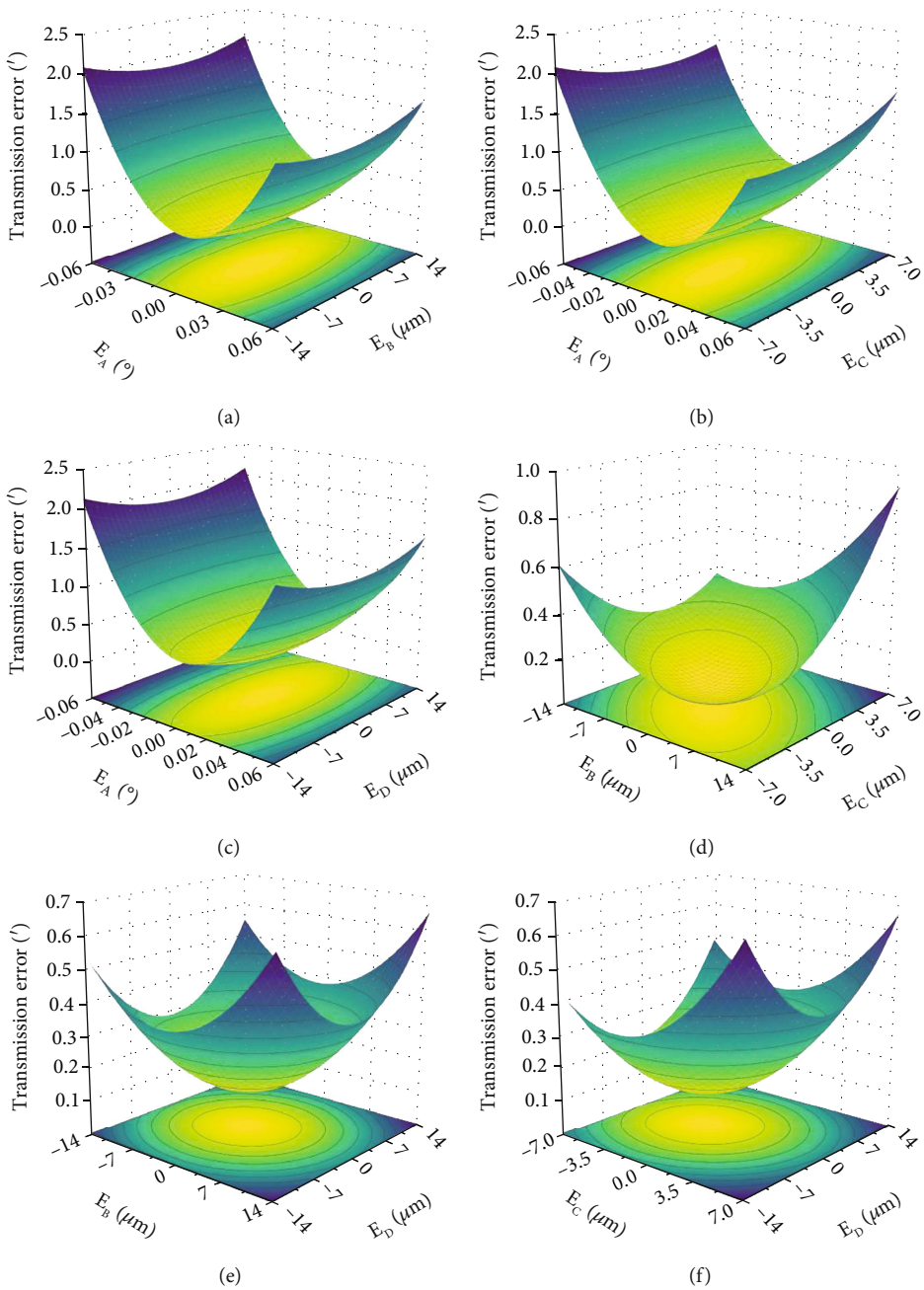

Figure 12: Response surfaces and contours.

of $R^2{}_{\text{adj}}$ are also high. Thus, the established response surface model has a high precision of prediction, which can be used to predict the transmission error of the RV reducer.

4.2.4. Analysis of Response Surfaces and Contours. To determine the effect of the interaction of the error factors on the transmission accuracy of the RV reducer, the response surfaces and contours of the interaction between the test factors are constructed, as shown in Figure 12.

The vertical projection of the response surface on the XY plane is the contour of the response surface model, and the shape of the contour line can visually show the significance of the interaction between the test factors, and the shape of the ellipse indicates a significant interaction, whereas the circle indicates an insignificant one.

The contour plot shown in Figure 12(a) does not form a closed ellipse, indicating that the interaction between E_A and E_B is not significant. Moreover, the corresponding response surface indicates that the slope of the surface changes significantly along the axial direction of E_A when E_B is given. Conversely, the slope of the surface changes slightly along the axial direction of E_B when E_A is given, indicating that E_A has more influence on the transmission error than E_B when the two interact. Similarly, in Figures 12(b) and 12(c), the

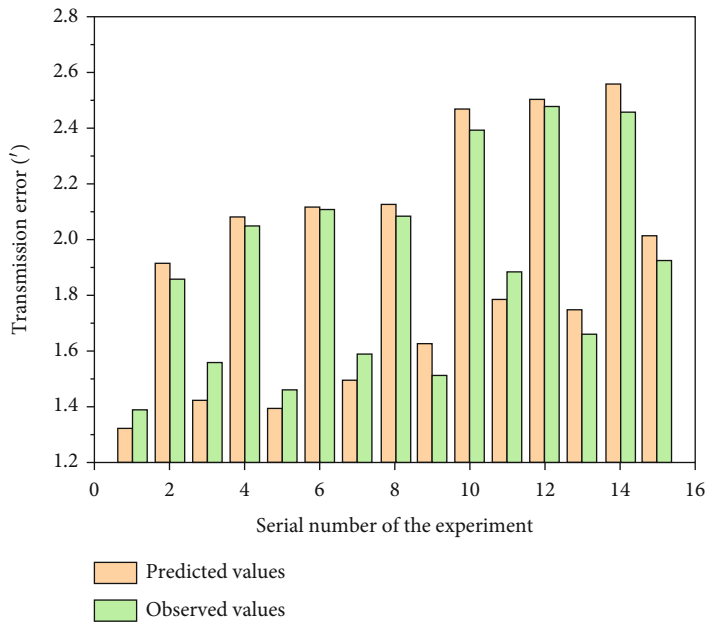

Figure 13: Comparison of predicted and observed values.

interaction between E_A and E_C is not significant, and E_A has the main effect on the transmission error. The interaction between E_A and E_D is not significant, and E_A has the main effect on the transmission error. The contour plot shown in Figure 11(d) tends to a sharp ellipse, indicating that the interaction between E_B and E_C is significant. The corresponding response surface shows that the slope of the surface changes along the axes of E_B and E_C with the same magnitude. The transmission error decreases with the decrease of E_B and the decrease of E_C forward deviation and the increase of reverse deviation, indicating that the influence of E_B and E_C on the transmission error is approximately equal. The contours shown in Figures 12(e) and 12(f) tend to be positively circular, indicating that the interaction between E_B and E_D is not significant. The interaction between E_C and E_D is also insignificant, as well as their respective relatively independent effects on the response of the transmission error.

The above response surface and contour analysis results correspond to the ANOVA results in Table 7, and the F value shows that the relationship between the degree of influence of the interaction between the factors on the transmission error of the RV reducer is $(E_B \times E_C) > (E_A \times E_C) > (E_A \times E_B) > (E_C \times E_D) > (E_A \times E_D) > (E_B \times E_D)$.

From the significance analysis in Table 7, the quadratic polynomial response surface function of the simplified RV reducer transmission error can be derived as

$$\begin{aligned}\gamma = {} & 0.12794 - 4.45389E_A + 2.258 \times 10^{-3}E_BE_C \\ & + 4.0436592 \times 10^2{E_A}^2 + 1.105 \times 10^{-3}{E_B}^2 \\ & + 4.15 \times 10^{-3}{E_C}^2 + 1.296 \times 10^{-3}{E_D}^2.\end{aligned} \tag{9}$$

To verify that the predicted values of the constructed quadratic regression equation about the transmission error of the RV reducer are in a reasonable range, 15 sets of models are constructed using the virtual prototype technique. The values of the four main error factors are randomly defined and given to these models for multibody dynamic simulations. The observed values of the simulation experiments are compared with the predicted values to check the accuracy of the response surface models. The predicted and observed values of the experiments are shown in Figure 13, in which the predicted values and the experimental results are extremely close to each other, thereby verifying the validity of the constructed response surface model.

In sum, the present work uses the RSM to analyze the effects of multiple error interactions on the transmission accuracy of the RV reducer and establish a response surface approximate model for intuitive and dynamic observation. In comparison with available conventional techniques, the method in this study better reveals the potential relationship between multiple error factors and the transmission error of the whole machine. In the future, the current work can be extended to the effect of multiple error factors on the friction in the cycloid-pin gear, as well as the effect on the reliability evolution of the RV reducer. Besides, in order to effectively achieve the research objectives of this article, some factors such as lubrication, wear, and temperature during the practical operation of the RV reducer are ignored in the construction of the model, which may lead to certain differences between the theoretical results and the actual test results. Therefore, how to improve the effectiveness of the constructed model is an important direction for our future research work. In the later work, we will further improve the model based on actual operating conditions and data of the RV reducer. In addition, with the development of intelligent algorithms, some advanced methods have been successfully applied to robot reducers [10, 11], and they will also provide new ideas and important references for our research work.

5. Conclusions

This study conducts simulations on the virtual prototype of the RV reducer. The results show that the errors associated with the involute planetary gear reducer mechanism in stage I have less interference with the transmission accuracy of the RV reducer. Conversely, the interaction of the errors existing in the cycloid-pin gear reducer mechanism in stage II has a greater effect on the transmission accuracy.

Subsequently, this study introduces the RSM into the analysis of the transmission accuracy of the RV reducer. In the single-factor test, the four error factors E_A, E_B, E_C, and E_D have significant effects on the transmission accuracy of the RV reducer under their individual effects. Therefore, an approximate model for analysis of the transmission accuracy of the RV reducer is constructed, with the four error factors as design variables and the transmission error as the response target. The analysis of the experimental results show that the combination of E_B and E_C has the greatest influence on the transmission accuracy of the RV reducer, and the value of the RV reducer transmission error decreases with the decrease of E_B and the decrease of E_C forward deviation and the increase of reverse deviation.

To sum up, the proposed method of analyzing the transmission accuracy of RV reducer based on RSM not only can improve the efficiency of calculation and analysis but also provides ideas for the subsequent efficient optimization of RV reducers.

Appendix

Total Transmission Ratio of RV Reducer

The transmission schematic of the RV reducer is shown in Figure 1, and the calculation process of its total transmission ratio is shown below.

The transmission ratio of the involute gear in stage I is

$$i_{12}^{7} = \frac{n_1 - n_7}{n_2 - n_7} = -\frac{Z_2}{Z_1}, \tag{A.1}$$

where n_1 is the speed of the input shaft, n_2 is the speed of the involute gear, n_7 is the speed of the output disk, Z_1 is the number of teeth of the sun gear, and Z_2 is the number of teeth of the involute gear.

The transmission ratio of the cycloid-pin gear in stage II is

$$i_{43}^{6} = \frac{n_4 - n_6}{n_3 - n_6} = 1 - \frac{n_4}{n_6} = \frac{Z_3}{Z_4}, \tag{A.2}$$

where n_3 is speed of the pin, n_4 is the speed of the cycloid gear, n_6 is the speed of the crankshaft, Z_3 is the number of teeth of the pin gear, and Z_4 is the number of teeth of the cycloid gear.

According to the transmission principle of the RV reducer, the speed of the crankshaft in stage II is the same as the speed of the involute gear in stage I, that is,

$$n_6 = n_2. \tag{A.3}$$

The speed of the output disk is the same as the revolution speed of the cycloid gear, that is,

$$n_7 = n_4. \tag{A.4}$$

By combining Equations (A.1)–(A.4) and substituting the corresponding values, the transmission ratio of the RV reducer can be expressed as follows:

$$i_{17} = \frac{n_1}{n_7} = 1 + \frac{Z_2 Z_3}{Z_1(Z_3 - Z_4)} = 121. \tag{A.5}$$

Data Availability

The data that support the findings of this study are available from the corresponding author upon reasonable request.

Conflicts of Interest

The authors declare that there is no conflict of interest regarding the publication of this paper.

Acknowledgments

This research has been supported by the National Natural Science Foundation of China (grant no. 52005004), the Anhui Provincial Natural Science Foundation (grant no. 2108085ME169), the National Key Laboratory of Science and Technology on Helicopter Transmission (grant no. HTL-O-22G01), the Key Research and Development Projects in Anhui Province (grant no. 2022a05020004), the Key Research and Development Projects in Zhejiang Province (grant no. 2021C01067), the Scientific Research Foundation for Talent Introduced (grant no. 2019YQQ005), and the Scientific Research Project of Anhui Polytechnic University (grant no. Xjky2020008).

References

[1] A. D. Pham and H. J. Ahn, "High precision reducers for industrial robots driving 4th industrial revolution: state of arts, analysis, design, performance evaluation and perspective," *International Journal of Precision Engineering and Manufacturing-Green Technology*, vol. 5, no. 4, pp. 519–533, 2018.

[2] B. Wei, J. X. Wang, G. W. Zhou, R. S. Yang, H. J. Zhou, and T. He, "Mixed lubrication analysis of modified cycloidal gear used in the RV reducer," *Proceedings of the Institution of Mechanical Engineers, Part J: Journal of Engineering Tribology*, vol. 230, no. 2, pp. 121–134, 2016.

[3] L. X. Xu, "A dynamic model to predict the number of pins to transmit load in a cycloidal reducer with assembling clearance," *Proceedings of the Institution of Mechanical Engineers, Part C: Journal of Mechanical Engineering Science*, vol. 233, no. 12, pp. 4247–4269, 2019.

[4] Y. H. Yang, C. Chen, and S. Y. Wang, "Response sensitivity to design parameters of RV reducer," *Chinese Journal of Mechanical Engineering*, vol. 31, no. 1, p. 49, 2018.

[5] L. X. Xu, B. K. Chen, and C. Y. Li, "Dynamic modelling and contact analysis of bearing-cycloid-pinwheel transmission

mechanisms used in joint rotate vector reducers," *Mechanism and Machine Theory*, vol. 137, pp. 432–458, 2019.

[6] H. Wang, Z. Y. Shi, B. Yu, and H. Xu, "Transmission performance analysis of RV reducers influenced by profile modification and load," *Applied Sciences*, vol. 9, no. 19, p. 4099, 2019.

[7] S. S. Jin, X. T. Tong, and Y. L. Wang, "Influencing factors on rotate vector reducer dynamic transmission error," *International Journal of Automation Technology*, vol. 13, no. 4, pp. 545–556, 2019.

[8] Y. H. Zhang, Z. Chen, and W. D. He, "Virtual prototype simulation and transmission error analysis for RV reducer," *Applied Mechanics and Materials*, vol. 789-790, pp. 226–230, 2015.

[9] H.-M. Qian, Y.-F. Li, and H.-Z. Huang, "Time-variant reliability analysis for industrial robot RV reducer under multiple failure modes using Kriging model," *Reliability Engineering and System Safety*, vol. 199, article 106936, 2020.

[10] I. Raouf, H. Lee, and H. S. Kim, "Mechanical fault detection based on machine learning for robotic RV reducer using electrical current signature analysis: a data-driven approach," *Journal of Computational Design and Engineering*, vol. 9, no. 2, pp. 417–433, 2022.

[11] I. Raouf, H. Lee, Y. R. Noh, B. D. Youn, and H. S. Kim, "Prognostic health management of the robotic strain wave gear reducer based on variable speed of operation: a data-driven via deep learning approach," *Journal of Computational Design and Engineering*, vol. 9, no. 5, pp. 1775–1788, 2022.

[12] B. K. Chen, C. Y. Li, T. C. Lim, X. Li, and Y. W. Wang, "Analysis of a cycloid speed reducer considering tooth profile modification and clearance-fit output mechanism," *Journal of Mechanical Design*, vol. 139, no. 3, article 033303, 2017.

[13] Y. Zhang, C. Y. Li, and J. Huang, "Transmission error analysis of cycloidal pinwheel based on muti-factor comprehensive effect," *Journal of Chongqing University*, vol. 43, no. 12, pp. 1–12, 2021.

[14] Y. H. Xie, L. X. Xu, and Y. Q. Deng, "A dynamic approach for evaluating the moment rigidity and rotation precision of a bearing-planetary frame rotor system used in RV reducer," *Mechanism and Machine Theory*, vol. 173, article 104851, 2022.

[15] J. G. Blanche and D. C. H. Yang, "Cycloid drives with machining tolerances," *Journal of Mechanisms, Transmissions, and Automation in Design*, vol. 111, no. 3, pp. 337–344, 1989.

[16] D. C. H. Yang and J. G. Blanche, "Design and application guidelines for cycloid drives with machining tolerances," *Mechanism and Machine Theory*, vol. 25, no. 5, pp. 487–501, 1990.

[17] H. J. Ahn, B. M. Choi, Y. H. Lee, and A. D. Pham, "Impact analysis of tolerance and contact friction on a RV reducer using FE method," *International Journal of Precision Engineering and Manufacturing*, vol. 22, no. 7, pp. 1285–1292, 2021.

[18] Z. H. Jiang, X. L. Zhang, and J. Q. Liu, "A reliability evaluation method for RV reducer by combining multi-fidelity model and Bayesian updating technology," *IOP Conference Series: Materials Science and Engineering*, vol. 1043, no. 5, article 052038, 2021.

[19] Y. H. Yang, G. C. Zhou, L. Chang, and G. Chen, "A modelling approach for kinematic equivalent mechanism and rotational transmission error of RV reducer," *Mechanism and Machine Theory*, vol. 163, article 104384, 2021.

[20] Y. H. Hu, G. Li, W. D. Zhu, and J. K. Cui, "An elastic transmission error compensation method for rotary vector speed reducers based on error sensitivity analysis," *Applied Sciences*, vol. 10, no. 2, p. 481, 2020.

[21] B. Schleich and S. Wartzack, "A discrete geometry approach for tolerance analysis of mechanism," *Mechanism and Machine Theory*, vol. 77, pp. 148–163, 2014.

[22] H. L. Nguyen and L. T. Duy, "Using the Box–Behnken response surface method to study parametric influence to improve the efficiency of helical gears," *Machines*, vol. 9, no. 11, p. 264, 2021.

[23] K. Huang, R. Xu, and Q. Chen, "Gear tolerance modeling with small displacement tosor and response surface method," *Journal of Xi'an Jiaotong University Xuebao*, vol. 51, pp. 77–84, 2017.

[24] H. Q. Wang, H. L. Wang, and J. X. Su, "Simulation analysis of RV reducer drive error based on ADAMS," *Machine Tool & Hydraulics*, vol. 49, pp. 135–140, 2021.

[25] G. A. Ambaye and H. G. Lemu, "Dynamic analysis of spur gear with backlash using ADAMS," *Materials Today: Proceedings*, vol. 38, pp. 2959–2967, 2021.

[26] Y. H. Xie, G. S. Chang, J. X. Yang, M. Y. Zhao, and J. Li, "Process optimization of robotic polishing for mold steel based on response surface method," *Machines*, vol. 10, no. 4, p. 283, 2022.

[27] W. C. Yan, X. Z. Meng, X. Cui, Y. L. Liu, Q. Chen, and L. W. Jin, "Evaporative cooling performance prediction and multi-objective optimization for hollow fiber membrane module using response surface methodology," *Applied Energy*, vol. 325, article 119855, 2022.

[28] F. Davoodi, M. Atapour, F. Ashrafizadeh, and R. Rikhtehgaran, "Dry sliding wear characteristics of NiP/TiN duplex coated aluminum alloy and wear analysis using response surface method," *Journal of Materials Engineering and Performance*, vol. 31, no. 8, pp. 6360–6372, 2022.